Supporting Information for:

***Title*:** Dysfunction of *GRAP*, Encoding the GRB2-Related Adaptor Protein, is Linked to Sensorineural Hearing Loss

Short title: *GRAP* Dysfunction is Linked to Hearing Loss

Chong Li, Guney Bademci, Asli Subasioglu, Oscar Diaz-Horta, Yi Zhu, Jiaqi Liu, Timothy Gavin Mitchell, Clemer Abad, Serhat Seyhan, Duygu Duman, Filiz Basak Cengiz, Suna Tokgoz-Yilmaz, Susan H. Blanton, Amjad Farooq, Katherina Walz, R. Grace Zhai, Mustafa Tekin

www.pnas.org/cgi/doi/10.1073/pnas.1810951115

Supplementary Tables

Table S1. Characteristics of 63 multiplex families from Turkey and Iran with autosomal recessive nonsyndromic HL in which all known deafness genes have been excluded. Parents are either consanguineous or originate from the same small town.

Family ID	# of affecteds	Exome Sequencing	Genome Sequencing	Family ID	# of affecteds	Exome Sequencing	Genome Sequencing
NSHL1	2	+	+	NSHL33	3	-	+
NSHL2	2	+	+	NSHL34	2	-	+
NSHL3	2	+	+	NSHL35	2	-	+
NSHL4	2	+	+	NSHL36	3	-	+
NSHL5	3	+	+	NSHL37	3	-	+
NSHL6	2	+	+	NSHL38	2	-	+
NSHL7	2	+	+	NSHL39	3	-	+
NSHL8	2	+	+	NSHL40	2	-	+
NSHL9	2	+	+	NSHL41	2	+	+
NSHL10	3	+	+	NSHL42	5	+	+
NSHL11	2	+	+	NSHL43	2	+	+
NSHL12	2	+	+	NSHL44	3	+	+
NSHL13	2	+	+	NSHL45	4	+	+
NSHL14	2	-	+	NSHL46	2	+	+
NSHL15	2	+	+	NSHL47	3	+	+
NSHL16	2	+	+	NSHL48	2	+	+
NSHL17	2	+	+	NSHL49	2	+	+
NSHL18	2	+	+	NSHL50	2	+	+
NSHL19	3	-	+	NSHL51	3	-	+
NSHL20	2	-	+	NSHL52	2	+	+
NSHL21	3	-	+	NSHL53	5	-	+
NSHL22	2	+	+	NSHL54	3	+	+
NSHL23	2	-	+	NSHL55	2	-	+
NSHL24	2	-	+	NSHL56	2	-	+
NSHL25	2	-	+	NSHL57	2	-	+
NSHL26	2	-	+	NSHL58	2	-	+
NSHL27	2	+	+	NSHL59	2	-	+
NSHL28	2	-	+	NSHL60	2	-	+
NSHL29	4	+	+	NSHL61	2	-	+
NSHL30	2	+	+	NSHL62	2	-	+
NSHL31	2	+	+	NSHL63	3	+	+
NSHL32	2	-	+				

Table S2. Parameters used for detecting homozygous runs by using exome Data (Enlis software).

Variation types to test	SNPs only
Ignore rare or common variations	<5% and >95%
Ignore variations that have a quality score less than	20
Consolidate nearby regions	Checked
Minimum region length	50000 bp
Window scan size	10 variations
Maximum number heterozygous variants in window scan	0
Percent of windows for homozygous position call	5%
Number of consecutive positions to call a homozygous region	15
Maximum gap between variations in a region	100000 bp

Table S3. Homozygous runs >1 Mb in the two probands of the families. Coverage of the entire region is given in whole genome sequencing data. Homozygous run containing *GRAP* is shown with red letters.

Family 1 individual II:1 coverages of homozygous regions				
#Chromosome Position (hg19)	Region Length	1X coverage	10X coverage	Average Read Depth
***17 : 26,079,849-34,869,155**	8,789,307	99.3	92	47.65
5 : 31,302,288-39,394,493	8,092,206	99.9	83.6	35.53
2 : 215,595,645-220,308,581	4,712,937	99.8	88.5	43.84
17 : 11,455,359-15,620,647	4,165,289	99.9	91.7	43.07
9 : 19,032,907-22,006,348	2,973,442	99.6	72.2	28.75
2 : 149,853,960-152,273,503	2,419,544	99.7	71.7	27.7
***17 : 18,394,431-20,354,836**	1,960,406	99	96.8	63.38
16 : 85,813,231-87,349,529	1,536,299	100	99.9	76.03
11 : 66,083,129-67,402,362	1,319,234	100	99.9	75.3
16 : 19,236,181-20,322,439	1,086,259	100	92.7	39.39
5 : 13,692,279-14,751,399	1,059,121	100	90.3	41.31
15 : 47,873,549-48,903,126	1,029,578	99.7	65	23.07
Family 2 individual II:1 coverages of homozygous regions				
#Chromosome Position (hg19)	Region Length	1X coverage	10X coverage	Average Read Depth
***17 : 27,225,399-34,869,155**	7,643,757	99.3	98.7	32.79
5 : 31,407,139-36,683,903	5,276,765	100	99.9	33.64
***17 : 18,397,711-20,354,836**	1,957,126	98.8	97.5	32.94
2 : 112,705,157-114,513,787	1,808,631	100	99.8	34.9
4 : 151,765,243-153,549,745	1,784,503	100	99.9	33.02
2 : 120,230,998-121,981,950	1,750,953	100	99.9	32.96
4 : 77,274,242-78,669,454	1,395,213	100	99.9	33.13
8 : 100,026,275-101,253,184	1,226,910	100	99.9	33.3
11 : 48,453,787-49,637,416	1,183,630	99.5	98.7	33.54
4 : 128,689,936-129,867,280	1,177,345	100	100	33.55
2 : 23,919,375-25,050,977	1,131,603	100	99.8	33.4
***17 : 26,079,849-27,187,636**	1,107,788	100	100	33.21
17 : 10,432,638-11,459,012	1,026,375	100	99.9	33.18

* Centromere of chr 17 is located between ~22-26 Mb

Table S4. Characteristics of the *GRAP* c.311A>T variant.

Gene	Transcript	c.DNA	protein	GnomAD allele freq	CADD Score	GERP RS	DANN Score	Provean	FATHMM
GRAP	NM_006613.3	c.311A>T	p.Gln104Leu	0.000004129	24	4.4499	0.9873	Damaging	Damaging

Table S5. Genotypes of SNP markers flanking the *GRAP c.311A>T*. *GRAP* variant and shared homozygous genotypes in two families are marked with red and brown letters, respectively.

dbSNP ID	gnomAD global Allele frequencies	Turkish population allele frequencies (41 control genomes)	Genomic position on chr17 (hg19)	Genomic Reference	Family 1 genotype	Family 2 genotype
rs62074238	0.4901	0.341463415	18314964	T	TG	TG
rs1682221	0.1048	0.353658537	18380065	C	CG	CG
rs1872344	0.3493	0.451219512	18394552	G	AA	AA
rs9709039	0.3574	0.426829268	18395647	G	TT	TT
rs1725645	0.3219	0.414634146	18397711	G	AA	AA
rs2305062	0.1331	0.073170732	18770530	A	GG	GG
rs2472715	0.3276	0.268292683	18880268	C	AA	AA
rs370564476	0.00000413	0	18927685	T	AA	AA
rs203462	0.3765	0.475609756	19812541	T	CC	CC
rs2108978	0.375	0.463414634	19861458	C	TT	TT
rs4925085	0.4904	0.56097561	20000131	G	TT	TT
rs201762600	0.1173	0.146341463	20361493	T	TC	TC
rs201278698	0.04383	0.134146341	20363552	C	CA	CA

Table S6. Sequences of primers/oligos used for the experiments.

Taqman Genotyping *GRAP* c.311A>T specific primer and reporter sequences		***amplicon***
***GRAP* Forward Primer**	5'-CACGCAGCACCTTGAAGTG-3'	54 bp
***GRAP* Reverse Primer**	5'-GGGTCCTTTCCCCTAGCTATG-3'	
***GRAP* Reporter 1 (VIC)**	5'-CTGCACCTGGTCTC-3'	
***GRAP* Reporter 2 (FAM)**	5'-TGCACCAGGTCTC-3'	
Mouse RT-PCR primer sequences		***amplicon***
***Grap* Forward**	5'-GAGGGTTTTGTTCCCAAGAA-3'	166 bp
***Grap* Reverse**	5'-TCACAGAGACGGAGAACTCG-3'	
***Gapdh* Forward**	5'-AGGTCGGTGTGAACGGATTTG-3'	129 bp
***Gapdh* Reverse**	5'-TGTAGACCATGTAGTTGAGGTCA-3'	
cDNA specific primer sequences for the splice experiments		
***GRAP*_cDNA_Forward**	5'-AGCCCCATCCGTGGTACT-3'	312 bp
***GRAP*_cDNA_Reverse**	5'-CCCCAGGTGACTTGAGCA-3'	
***GRAP* exon 4 specific primer sequences**		
***GRAP* ex4 Forward**	5'-AGACAGGCTGGTTCCAGGT-3'	383 bp
***GRAP* ex4 Reverse**	5'-GCTGCTGGGGAAGTGAGA-3'	

Table S7. List of rare *MYO15A* variants (<0.05 global allele frequency in gnomAD) mapping to chr17:18,012,020-18,083,116 (hg19) in probands of both families. No copy number or structural variants were detected involving *MYO15A*. These data are from whole genome sequencing.

Position	Type	Ref	Var*	Region	Variant**	GERP RS	CADD	GnomAD allele freq
18020144	SNP	G	C	INTRON	c.-219-1752G>C	0.2349	4.375	-
18028608	SNP	G	A	INTRON	c.3756+63G>A	-5.63	1.996	0.00003231
18081676	DEL	C	-	INTRON	c.10492-407delC	-0.4589	0.280	-

*all variants are homozygous

** transcript: NM_016239.3

Supplementary Figures

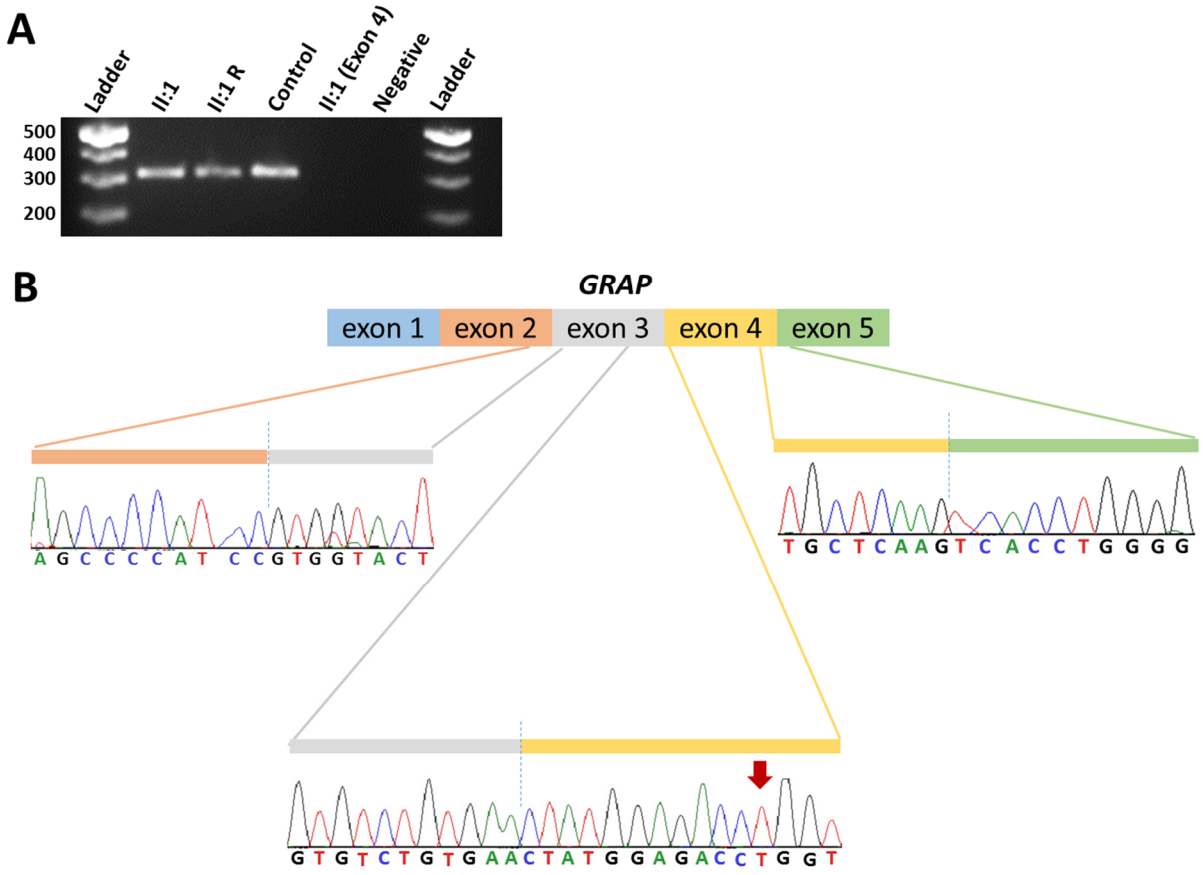

Figure S1. No effect of *GRAP* c.311A>T on splicing. (A) RT-PCR from saliva samples of the affected individual II:1 in family 1 and a control individual shows the same bands at expected size (312 bp). II:1 R is repeat RT-PCR from individual II:1. II:1 (exon 4) is the negative result of an intronic primer. **(B)** Sanger sequencing shows intact exon-exon boundaries (vertical dotted lines). Red arrow indicates the c.311A>T variant.

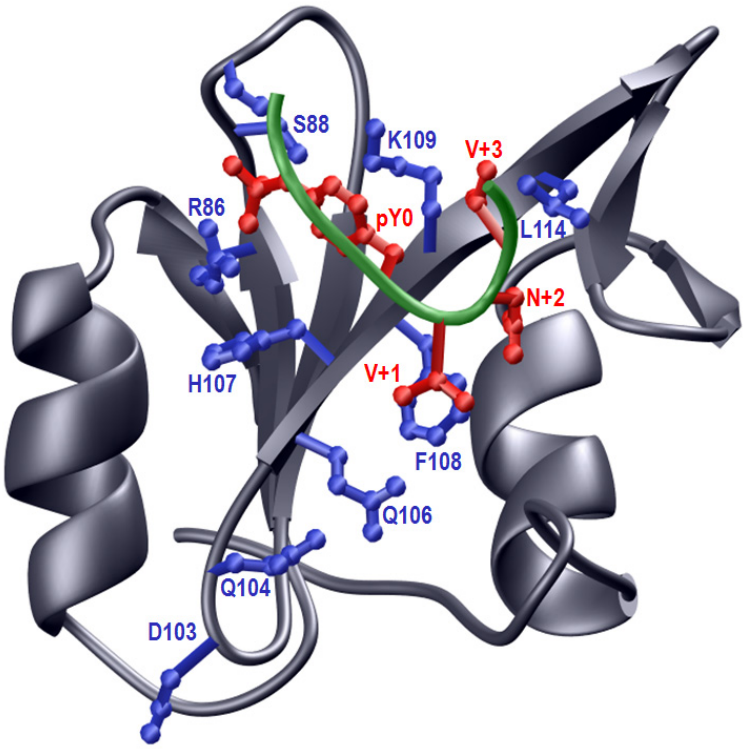

Figure S2. Ribbon representation of the structural model of the SH2 domain of human GRAP complexed to a tyrosine-phosphorylated (pY) peptide harboring the consensus pYVNV sequence. The SH2 domain of GRAP adopts a classical β-sandwich fold that is broadly comprised of a central antiparallel β-sheet sandwiched between α-helices on each side. The peptide docks orthogonally relative to the central β-sheet along one face of the β-sandwich. In this manner, the pY and the following three residues within the pYVNV sequence of the peptide are able to engage in numerous intermolecular interactions with their counterparts within the SH2 domain. The backbones of SH2 domain and the bound peptide are colored gray and green, respectively. The sidechain moieties of residues in SH2 domain lining the peptide-binding pocket and those located at positions 103/104 are colored blue. The sidechain moieties of residues in the peptide that interact with the residues lining the peptide-binding pocket in SH2 domain are colored red. In the peptide, residues following the pY in the pYVNV sequence are labeled V+1, N+2, and V+3 relative to pY, which is arbitrarily assigned a 0 (pY0).

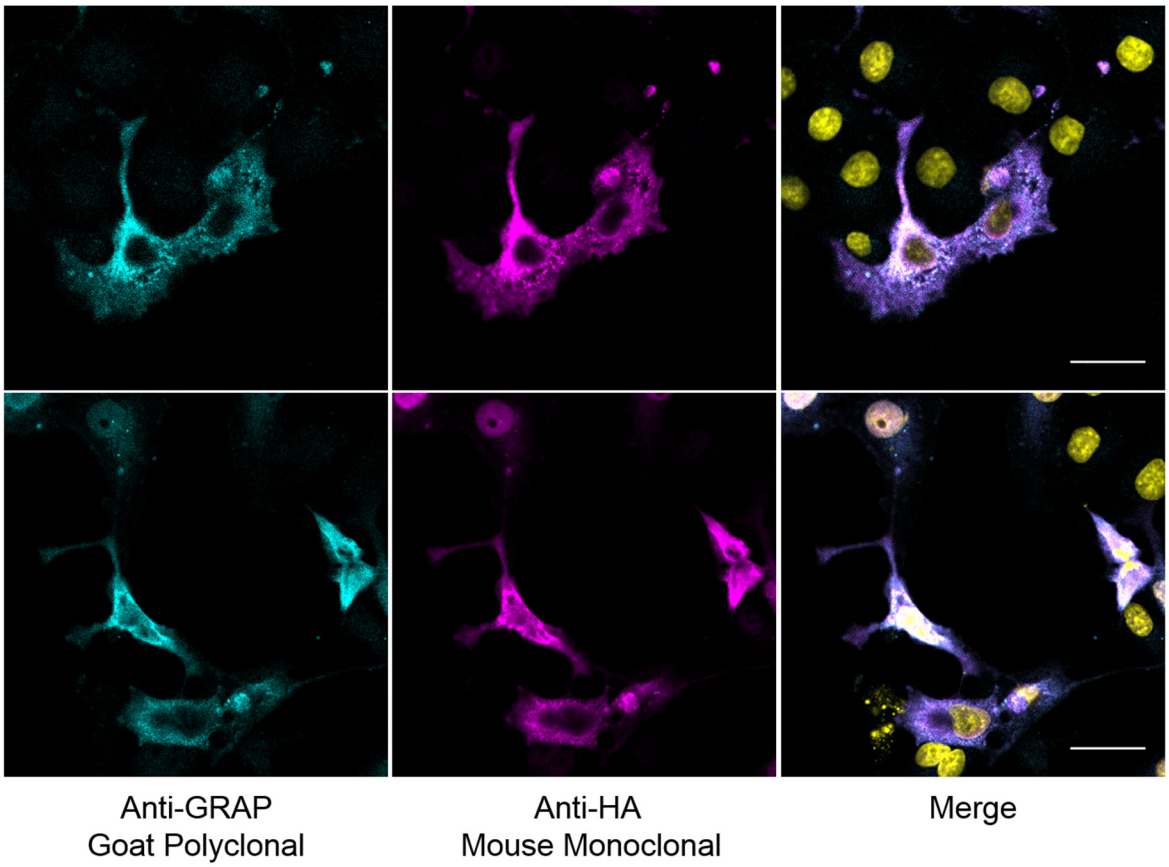

Figure S3. Validation of the GRAP antibody. In transfected COS-7 cells, magenta (anti-HA) and cyan (anti-GRAP) signals corresponding to both primary antibodies show identical staining patterns that overlap in the Merge + DAPI (yellow) panels. Scale bar, 30 μm.

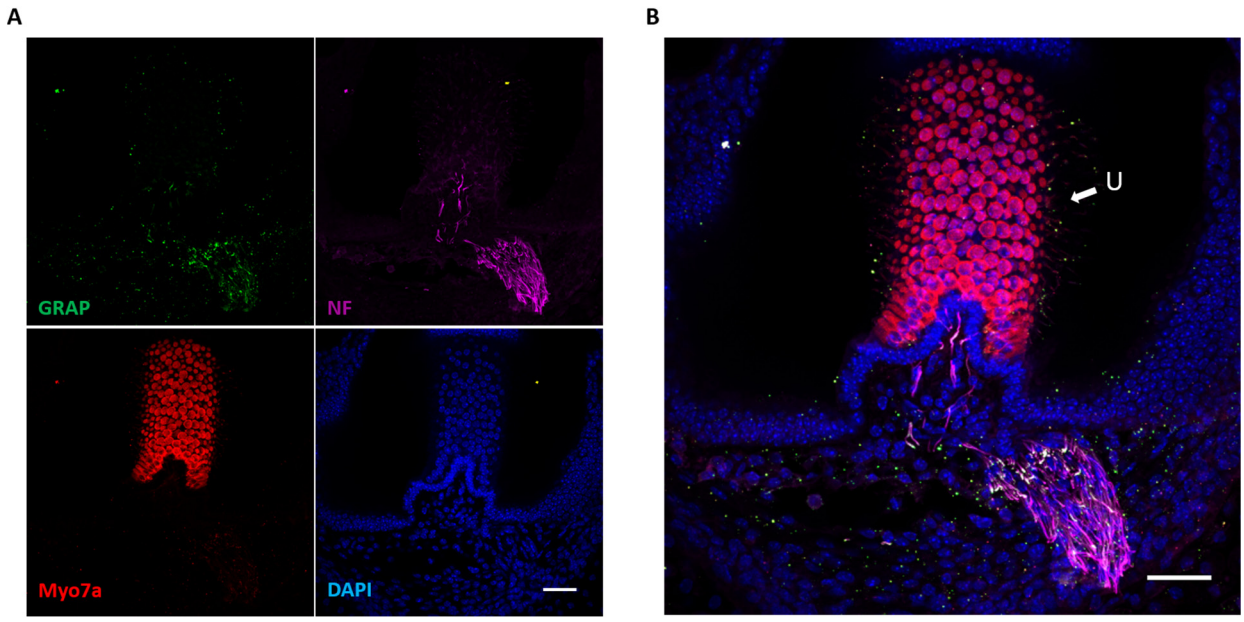

Figure S4. Grap localization in the mouse utricle. (A) Representative z-stack projection staining of P0 utricle whole mount stained for neurofilament heavy chain (NF) to reveal the total innervation pattern (purple), antibody to Grap (green); Myo7a (red) to stain the utricle hair cells and DAPI (blue). Note the localization of Grap at the length of the nerves. Scale bar, 40 μm. **(B)** Merged image of Grap, Myo7a, DAPI and NF. Arrow indicates utricle (U); Scale bar, 40 μm.

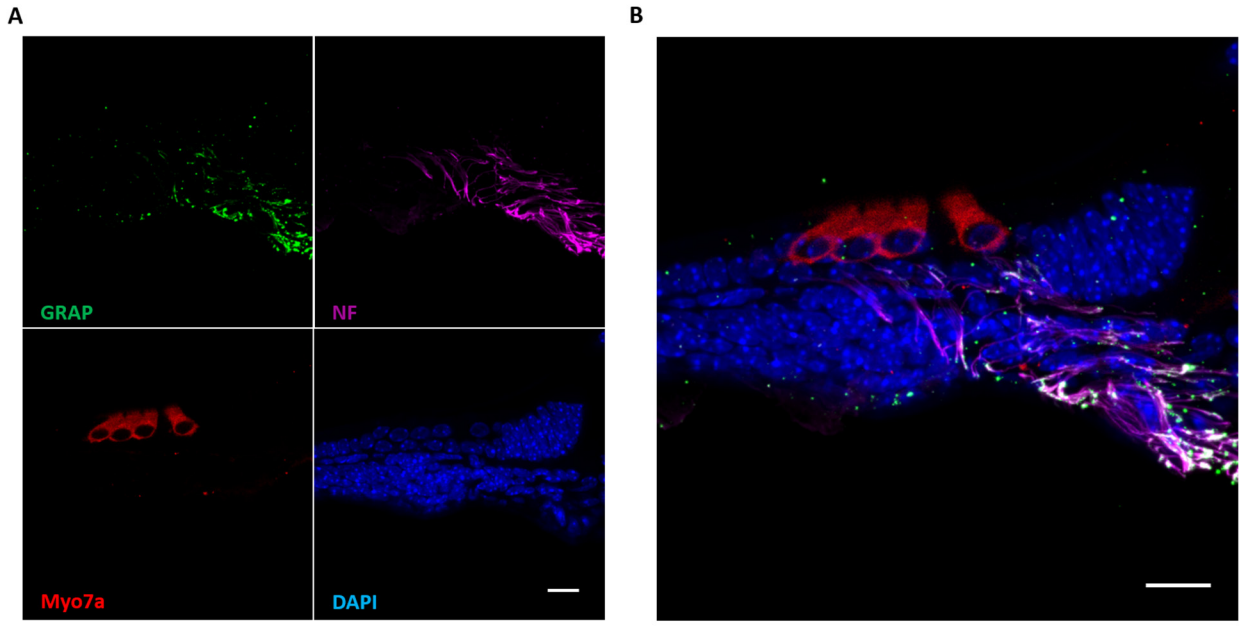

Figure S5. Grap localization in the mouse cochlea. (A) Representative z-stack projection staining of P0 cross section of cochlea stained for neurofilament heavy chain (NF) to reveal the total innervation pattern (purple), antibody to Grap (green); Myo7a (red) to stain the hair cells and DAPI (blue). Note the localization of Grap at the length of the nerves. Scale bar, 40 µm. **(B)** Merged image of Grap, Myo7a, DAPI and NF. Scale bar, 40 µm.

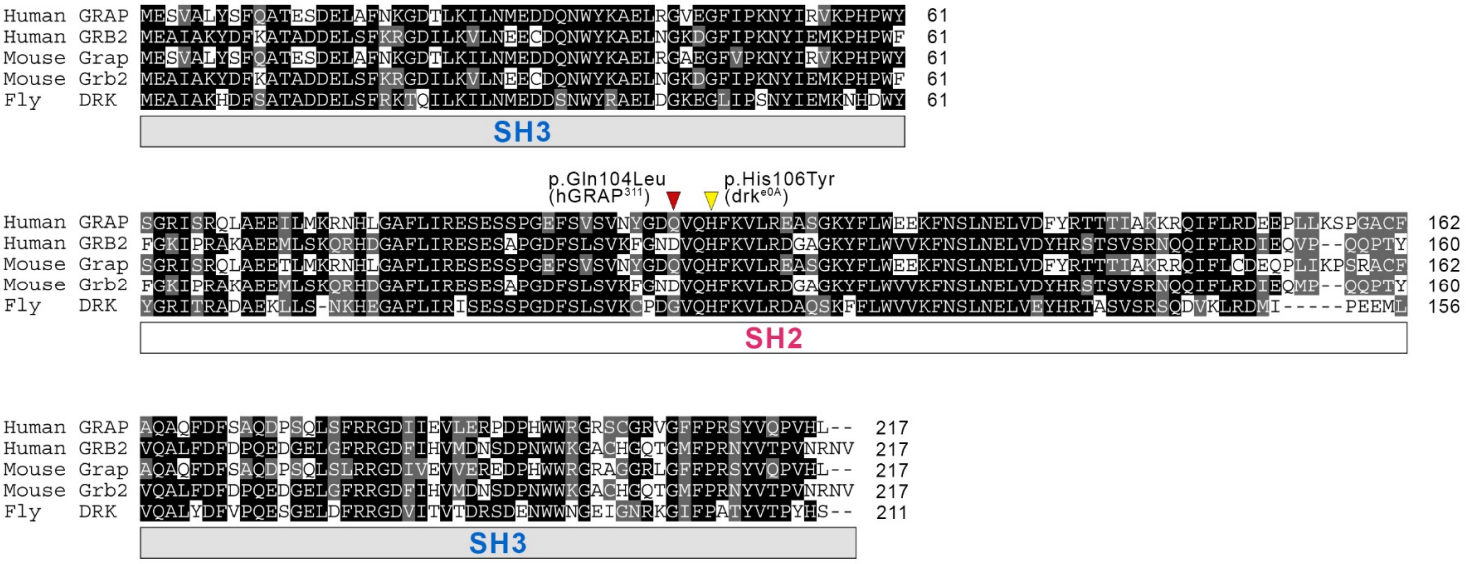

Figure S6. Protein sequence alignment showing evolutionary conservation of GRAP/GRB2/drk proteins.

Black background indicating identical amino acid, grey background indicating similar amino acid, and the rest of the amino acids are indicated by white background. Red arrow head indicates the mutation identified in human patients with nonsyndromic hearing loss. Yellow arrow head indicates a *Drosophila* mutant allele.

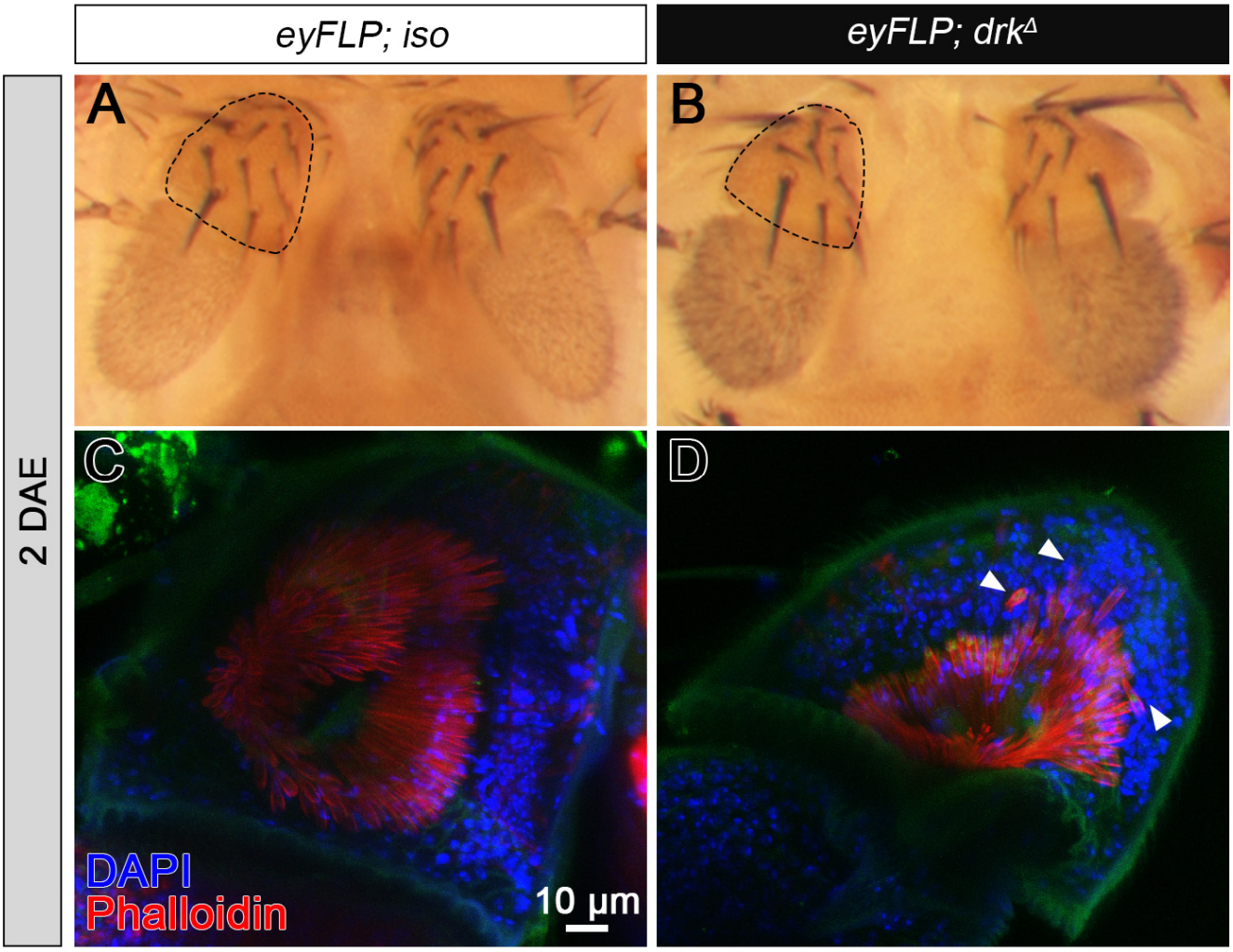

Figure S7. Loss of drk in JO causes disorganized morphology of the scolopidia in the mosaic animals. (A-B) Antennae of 2 DAE female flies. Black dashed outline labels JO. **(C-D)** Confocal micrographs show the morphology of actin bundles in the scolopidium. DAPI labels nuclei, and phalloidin labels cap rods, scolopale rods and actin bundles in the cilium. White arrowheads indicate disorganized structure stained by phalloidin.

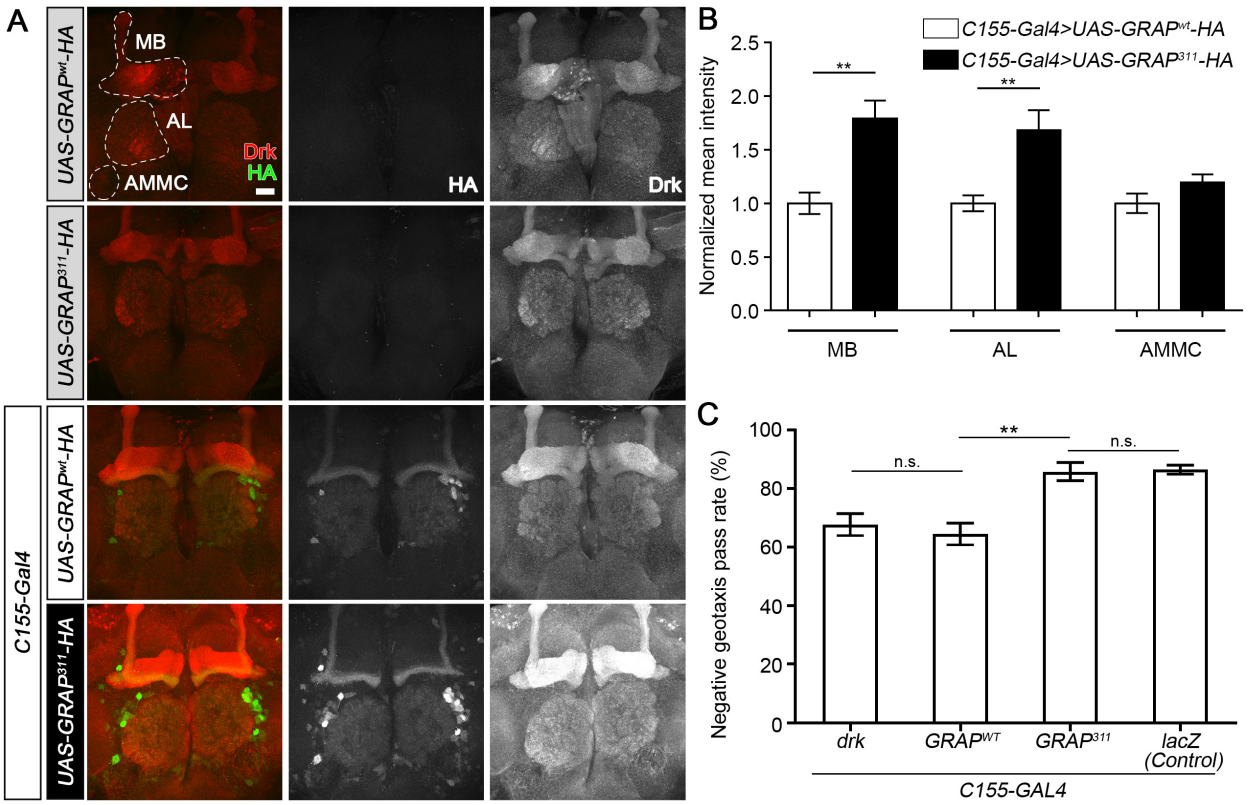

Figure S8. Neuronal expression of wild type and mutant GRAP have different effects on endogenous drk levels and climbing deficits. (A) Confocal micrographs of the fly brains overexpressing HA-tagged wild type or mutant GRAP proteins using *C155-GAL4* driver. MB, mushroom body; AL, antenna lobe; AMMC, antennal mechanosensory motor center. **(B)** Quantification of drk levels in different regions of the brain (mean ± S.E.M.; n = 5 sections (MB), and 6 sections (AL and AMMC)). **(C)** Negative geotaxis performance [mean ± S.E.M.; each data point obtained from a group of 10 individuals, n = 10 experiments] female flies at 2 DAE. Scale bar, 20 µm. One-way ANOVA post hoc Tukey test. ***P* < *0.01*.

Supplementary Materials and Methods

Statement of ethics

This study was approved by the University of Miami Institutional Review Board (USA) and the Ankara University Medical School Ethics Committee (Turkey). A signed informed-consent form was obtained from each participant or, in the case of a minor, from the parents.

Human subjects

Detailed past medical histories and a thorough physical exam including otoscopy and ophthalmoscopy revealed no abnormalities and an electrocardiogram was unremarkable.

DNA Sequencing and bioinformatics

Exome sequencing was performed on probands (family 1 II:1 and family 2 II:1) of the families by using a previously published protocol (1). Variants were filtered by Genesis 2.0 (https://www.genesis-app.com/). For the variant allele frequency filtering EVS (http://evs.gs.washington.edu/EVS/), gnomAD (http://gnomad.broadinstitute.org/), dbSNP (https://www.ncbi.nlm.nih.gov/projects/SNP/) databases as well as our internal exome database that includes > 4,000 exomes from different ethnicities including > 500 Turkish individuals were used. Minor allele frequency thresholds of 0.005 for recessive and 0.0005 for dominant variants were used as recommended (2). We used GERP > 2 for conservation (3). We also filtered variants by using criteria of CADD Score > 20 (4) DANN score > 0.95 (5) and damaging for Provean (http://provean.jcvi.org/index.php) and FATHMM (http://fathmm.biocompute.org.uk/) for missense variants. XHMM and Conifer were used for the Copy Number Variant detection (6). Sanger sequencing is used for confirmation and co-segregation of the variant. Enlis Genome Research software (https://www.enlis.com/) was used to identify homozygous regions from WES data.

For comprehensive variant screening of protein-coding as well as noncoding regions, genome sequencing was also performed in the both probands of the families by using an Illumina Hiseq X Ten platform at HudsonAlpha. Reads were mapped to the human reference genome (NCBI build37/hg 19 version) and variants were called according to standard protocols (7-10). Copy number variants were called using the CNVnator (11).

Structural modeling

Structural model of SH2 domain (residue 58-152) of human GRAP in complex with a tyrosine-phosphorylated (pY) peptide was built using the MODELLER software based on homology modeling (12). Briefly, the crystal structure of the homologous SH2 domain of human GRB2 (PDBID 1JYR) bound to a tyrosine-phosphorylated (pY) peptide was used as a template (13). It should be noted that the SH2 domains of GRAP and GRB2 share over 60% sequence identity at amino acid level as determined by pairwise sequence alignment using Clustal Omega (14). With such high level of sequence identity between the template and model, the structural model presented here can be relied upon with a very high degree of confidence. A total of 100 atomic models were calculated and the structure with the lowest energy, as judged by the MODELLER Objective Function, was selected for further analysis. The structural model was rendered using RIBBONS (15).

TaqMan SNP Genotyping

We used a custom TaqMan SNP assay from Applied Biosystems (Assay ID: AHABHEF; order date: 09/22/2014) specific to GRAP c.311A>T variant to screen 690 probands from unrelated families with NSHL. Custom-designed TaqMan SNP Genotyping Assays were designed to identify the presence or absence of the variant (*SI Appendix*, Table **S6**). Samples were amplified for 40 cycles then the plates were

read on the 7900HT Fast Real-Time PCR instrument (Applied Biosystems, Foster City, CA). Finally, data were analyzed by using the SDS v2.4 software.

Studied mice

Wild type C57Bl/6 mice were bred and maintained at the University of Miami. At weaning age, mice were housed 2-4 per cage in a room with a 12 hour light: dark cycle (lights on at 7 AM, off at 7 PM) with access to food and water *ad lib*. All procedures were approved by the University of Miami Institutional Animal Care and followed the NIH Guidelines, "Using Animals in Intramural Research".

RT-PCR

To check the expression of *Grap* in different tissues, lung, liver, kidney, brain and cochlea were dissected from P_{15} wild type mice. In addition, cochlear expression of *Grap* was checked in embryos of 17.5 dpc. Total RNA was isolated with TRIzol Reagent (Invitrogen) according to manufacturer's instructions. Prior to reverse transcription, RNA samples were treated with rDNAse I (DNA-free kit, Applied Biosystems). cDNA was synthetized using qScript XLT cDNA SuperMix (Quanta Biosciences) (*SI Appendix*, Table **S6**).

Saliva samples from patient and control collected by using Oragene®•RNA Re-100 kit (DNA genotek). RNA was extracted by using manufacturer protocol and cDNA was synthetized using qScript XLT cDNA SuperMix (Quanta Biosciences) (*SI Appendix*, Table **S6**).

Immunofluorescence

Tympanic bullae containing the cochleae were dissected from P_0 mice under the microscope and locally perfused with 4% PFA through the round and oval windows. Samples were kept in 4% PFA at 4 °C overnight and rinsed in 1X PBS. Cochleae whole mounts were permeabilized with 0.5% Triton X-100 and blocked in 5% BSA for 1 hour at room temperature, followed by overnight incubation at 4 °C with primary antibodies. Goat anti-Grap polyclonal antibody (Abcam, ab9703) was utilized as primary antibody. Co-staining was performed with anti-neurofilament, heavy chain, (Millipore, AB5539) and DAPI. Images were captured with a Zeiss LSM710 confocal microscope.

Validation of the GRAP antibody

Cos-7 cells were transfected with mammalian expression plasmids encoding for human GRAP with an in frame HA tag in the c-terminus (Genecopoeia). After 48-hour incubation, cells were fixed, permeabilized, and blocked with PBS-BSA 5% solution. Primary antibodies consisted of an anti-GRAP goat polyclonal antibody (Abcam, ab9703) and a mouse monoclonal anti-HA antibody (Cell Signaling Technology, mAb #2367). The immunogen consisted on a peptide corresponding to C terminal amino acids 205-217 of human GRAP (*SI Appendix*, Figure **S3**).

***Drosophila* stocks and genetics**

Flies are maintained on a cornmeal-molasses-yeast medium at 25°C, 65% humidity, 12 h light/ 12 h dark. The following fly strains were used in the studies: $drk^{14\text{-}7}$ (27622), drk^{6} (27623), drk^{e0A} (5691), *actin-GAL4, FRT42Diso, eyFLP; FRT42D,* w^{+}, cl^{-}, obtained from Bloomington *Drosophila* Stock Center; $drk^{\Delta P24}$ (named as drk^{Δ} in this study) from Dr. Skoulakis's lab. All *drk* alleles were normalized to the w^{-} background and balanced with *Cyo, KrGFP* chromosome. For mosaic analysis, drk^{Δ} was recombined with the *FRT42Diso* chromosome.

Complementation analysis and survival experiments

Young (2-5 DAE) male and virgin female flies were selected as parental flies for crossing 24 hours. Flies were then transferred to new vials and allowed to lay eggs for 4-6 hours (~ 100-150 embryos in each vial).

For each sex, percent survival to adulthood was calculated using the following formula and presented as the average of both sexes:

$$Percent\ survival = \frac{2\ X\ Number\ of\ compound\ heterozygous}{Number\ of\ CyO\ flies}$$

Negative geotaxis behavior assay

Climbing behavior was measured as previously described (16). Briefly, nine or ten age matched female flies for each genotype were placed in a vial marked with an 8 cm line from the bottom surface. The flies were tapped gently onto the bottom and given 10 s to climb. The number of flies that successfully climbed above the 8 cm marked within 10 seconds was recorded and divided by the total number of flies. The assay was repeated 10 times, and more than 5 independent groups (indicated in the results) from each genotype were tested.

Immunofluorescent staining of fly tissues

For cryosections of JO, fly heads were cut in cold PBS and the proboscis was removed. Heads were fixed in fresh made 4% formaldehyde (in PBS) with 0.01% PBTx for 60 min in 4 °C and then washed with PBS twice, 5 min each time. Next, heads were transferred to 12% sucrose with 0.01% PBTx and incubated overnight at 4 °C. Heads were then transferred to molds filled with Optimal Cutting Temperature (O.C.T.) compound (Tissue-Tek, 4583) and allowed to freeze for 40s using dry ice/ethanol bath. Samples were cryosectioned at 12 μm, dried at room temperature for 30 min and fixed with 0.5% formaldehyde for 20 min. Slides were then rinsed with PBS three times and 0.4% PBTx five times. The slides were then incubated with primary antibodies diluted in 0.4% PBTx containing 5% goat serum overnight at 4 °C. Slides were then incubated at room temperature with conjugated secondary antibodies for 2h, followed by staining with DAPI for 10 min. After washing, tissues were mounted with VECTASHIELD Antifade Mounting Medium (Vector Laboratories) and kept at 4 °C until imaging. For whole mount of JO, the antennae were detached from the heads and fixed in fresh made 4% formaldehyde (in PBS) with 0.01% PBTx for 20 min. The antennae were then washed with 0.4% PBTx for three times followed by same immunostaining protocol as cryosections. The following primary and secondary antibodies are used in this study: anti-drk (from Dr. Skoulakis's lab), anti-Brp (DSHB, AB_2314866), anti-Csp (DSHB AB_528183), anti-synapsin (DSHB, AB_2313867), anti-HA (6E2, Cell Signaling 2367) Cy5 conjugated anti-HRP (123175021, Jackson ImmunoLab), Alexa 546 conjugated phalloidin (ThermoFisher Scientific, A22283), Cy5 conjugated anti-HRP and secondary antibodies conjugated to Alexa 488/568/647 (ThermoFisher Scientific).

Multiple sequence alignment and heatmap

For the multiple sequence alignment in Figure 1D, the following versions of the GRAP protein are used: Homo sapiens (Version: CAG46739.1), Macaca mulatta (Version: NP_001244988.1), Mus musculus (Version: NP_082093.1), Bos taurus (Version: AAI47999.1), Delphinapterus leucas (Version: XP_022416511.1), Pteropus alecto (Version: ELK15742.1), Danio rerio (Version: AAI64308.1), and Gallus gallus (Version: NP_001264482.1), Geospiza fortis (Version: XP_014164548.1), and Lonchura striata domestica (XP_021406213.1) (https://www.ncbi.nlm.nih.gov/protein/).

Multiple sequence alignment in Figure 3B was performed using ClustalW and Multiple Align Show. The following sequences are used: Human GRAP (NP_006604.1), Human GRB2 (NP_002077.1), Mouse Grap (NP_082093.1), Mouse Grb2 (NP_032189.1), and *Drosophila* drk (NP_476858.1). Heatmap was generated using the ggplot2 package in RStudio.

Statistics

Data were analyzed with Prism (GraphPad Software). Student's *t* test (two tailed) was used for comparison of two groups. One-way ANOVA with Tukey ($n \geq 5$) correction was used for comparison of

more than two group. $P < 0.05$ was considered statistically significant. Single locus two-point LOD scores were calculated using Superlink Online SNP 1.1 with a disease allele frequency of 0.0001 under a fully penetrant autosomal recessive model (17).

Supporting References

1. Bademci G*, et al.* (2016) Comprehensive analysis via exome sequencing uncovers genetic etiology in autosomal recessive nonsyndromic deafness in a large multiethnic cohort. *Genet Med* 18(4):364-371.
2. Shearer AE*, et al.* (2014) Utilizing ethnic-specific differences in minor allele frequency to recategorize reported pathogenic deafness variants. *Am J Hum Genet* 95(4):445-453.
3. Cooper GM*, et al.* (2005) Distribution and intensity of constraint in mammalian genomic sequence. *Genome Res* 15(7):901-913.
4. Kircher M*, et al.* (2014) A general framework for estimating the relative pathogenicity of human genetic variants. *Nature Genet* 46(3):310-315.
5. Quang D, Chen Y, & Xie X (2015) DANN: a deep learning approach for annotating the pathogenicity of genetic variants. *Bioinformatics* 31(5):761-763.
6. Bademci G*, et al.* (2014) Identification of copy number variants through whole-exome sequencing in autosomal recessive nonsyndromic hearing loss. *Genet Test Mol Biomarkers* 18(9):658-661.
7. Bowling KM*, et al.* (2017) Genomic diagnosis for children with intellectual disability and/or developmental delay. *Genome Med* 9(1):43.
8. DePristo MA*, et al.* (2011) A framework for variation discovery and genotyping using next-generation DNA sequencing data. *Nature Genet* 43(5):491-498.
9. Li H & Durbin R (2010) Fast and accurate long-read alignment with Burrows-Wheeler transform. *Bioinformatics* 26(5):589-595.
10. McKenna A*, et al.* (2010) The Genome Analysis Toolkit: a MapReduce framework for analyzing next-generation DNA sequencing data. *Genome Res* 20(9):1297-1303.
11. Abyzov A, Urban AE, Snyder M, & Gerstein M (2011) CNVnator: an approach to discover, genotype, and characterize typical and atypical CNVs from family and population genome sequencing. *Genome Res* 21(6):974-984.
12. Marti-Renom MA, *et al*. (2000) Comparative protein structure modeling of genes and genomes. Annu Rev Biophys Biomol Struct 29: p. 291-325.
13. Nioche P, *et al*. (2002) Crystal structures of the SH2 domain of Grb2: highlight on the binding of a new high-affinity inhibitor. J Mol Biol 315(5): p. 1167-77.
14. Sievers F, *et al*. (2011) Fast, scalable generation of high-quality protein multiple sequence alignments using Clustal Omega. Mol Syst Biol 7: p. 539.
15. Carson M (1991) Ribbons 2.0. J Appl Crystallogr 24: p. 958-961.
16. Li C, *et al*. (2017) Spermine synthase deficiency causes lysosomal dysfunction and oxidative stress in models of Snyder-Robinson syndrome. Nat Commun 8(1):1257.
17. Silberstein M, *et al*. (2013) A system for exact and approximate genetic linkage analysis of SNP data in large pedigrees. Bioinformatics 29(2):197-205.